COMMUNICATION

Glucose Binding Drives Reconfiguration of a Dynamic Library of Urea-Containing Metal-Organic Assemblies

Dong Yang,[a, b] Larissa K. S. von Krbek,[a,c] Le Yu,[b] Tanya K. Ronson,[a] John D. Thoburn,[d] John P. Carpenter,[a] Jake L. Greenfield,[a] Duncan J. Howe,[a] Biao Wu,[b] and Jonathan R. Nitschke[a]*

[a] D. J. Howe, Dr. D. Yang, Dr. L. K. S. von Krbek, Dr. T. K. Ronson, Dr. J. P. Carpenter, Dr. J. L. Greenfield, Prof. J. R. Nitschke
Department of Chemistry
University of Cambridge
Lensfield Road, Cambridge, CB2 1EW, United Kingdom
E-mail: jrn34@cam.ac.uk

[b] Dr. D. Yang, Prof. L. Yu, Prof. B. Wu
Key Laboratory of Synthetic and Natural Functional Molecule of the Ministry of Education
College of Chemistry and Materials Science
Northwest University
Xi'an 710069, China

[c] Dr. L. K. S. von Krbek,
Present address: Kekulé-Institut für Organische Chemie und Biochemie, Rheinische Friedrich-Wilhelms-Universität Bonn
Gerhard-Domagk-Str. 1, 53121 Bonn, Germany

[d] Prof. J. D. Thoburn
Department of Chemistry
Randolph-Macon College
Ashland, Virginia 23005, United States

Supporting information for this article is given via a link at the end of the document.

Abstract: A bis-urea-functionalized ditopic subcomponent assembled with 2-formylpyridine and Fe^{II}, resulting in a dynamic library of metal-organic assemblies: an irregular $Fe^{II}_4L_6$ structure, and three $Fe^{II}_2L_3$ stereoisomers: left- and right-handed helicates and a *meso*-structure. This library reconfigured in response to the addition of monosaccharide derivatives, which served as guests for specific library members, and the rate of saccharide mutarotation was also enhanced by the library. The (*P*) enantiomer of the $Fe^{II}_2L_3$ helical structure bound β-D-glucose selectively over α-D-glucose. As a consequence, the library collapsed into the (*P*)-$Fe^{II}_2L_3$ helicate following glucose addition. The α-D-glucose was likewise transformed into the β-D-anomer during equilibration and binding. Thus, β-D-glucose and (*P*)-**3** amplified each other in the product mixture, as metal-organic and saccharide libraries geared together into a single equilibrating system.

Discrete molecular containers have found uses in catalysis,[1] guest recognition and separation,[2] drug delivery,[3] gas absorption and storage,[4] as well as sensing.[5] Metal-organic cages in particular have found wide uses, due to their versatile and tunable host–guest chemistry, straightforward synthetic accessibility, structural adaptability and stimuli-responsive transformations.[4b, 6]

Hydrogen-bonding is widely used for molecular recognition and self-assembly, such as the formation of gels using a series of rigid bis(urea) building blocks,[7] the construction of anion-coordination-based tetrahedral cages and triple helices,[8] the generation of a hydrogen-bonded octameric nanospheroid,[9] a cryptand-like cage that uses only C-H···X^- hydrogen bonding to trap chloride with exceptional affinity,[10] and covalent organic cages for monosaccharide[11] or anion[12] binding.

Self-assembled metal-organic cage walls are usually constructed from rigid aromatic panels. The hydrophobic effect, coulombic interactions, aromatic stacking, and ion-π interactions thus often serve as the principal driving forces for guest binding. Examples of metal-organic cages with hydrophilic cavities or functional groups for hydrogen bonding within the cavity are therefore noteworthy.[13] Custelcean and co-workers designed urea-functionalized $M^{II}_4L_6$ cage receptors for the selective encapsulation of tetrahedral oxoanions from aqueous solution.[14] Kaifer *et al.* reported urea-containing subcomponent self-assembled $M^{II}_4L_6$ tetrahedral metal–organic cages which combined high binding affinities for sulfate with straightforward release through cage disassembly.[15] Sun's group described a self-assembled $Pd^{II}_2L_4$ cage which selectively encapsulates nitrate.[16] The Fujita group decorated the interior of an $M^{II}_{12}L_{24}$ spherical cage with peptides to form a protein-mimetic cavity.[17] Reek et al. functionalized this spherical cage framework with guanidinium units, and used it to pre-organize catalysts and substrates for highly efficient reactions.[18]

Here we report a strategy for generating metal-organic cages capable of forming hydrogen bonds with guest molecules. As shown in Figure 1, ditopic aniline subcomponent **A**, containing two urea units, assembled with 2-formylpyridine and iron(II) bis(trifluoromethanesulfon)imide (triflimide, Tf_2N^-) to form a dynamic library[19] containing an irregular $Fe^{II}_4L_6$ structure (**1**) and three $Fe^{II}_2L_3$ stereoisomers.[20] These structures have multiple urea hydrogen-bond donors capable of interacting with guests.

Irregular **1** interconverted with higher-symmetry **2** and **3**, with the equilibria between structures influenced by the presence of competent guests. The addition of β-D-glucose or methyl β-D-glucoside led to near-complete transformation of all library members into (*P*)-helicate **3**, because these guests bound to (*P*)-**3** an order of magnitude more strongly than to (*M*)-**3** or **2**. Furthermore, binding of α-D-glucose and β-D-glucose significantly accelerated mutarotation between the two anomers, as described below.

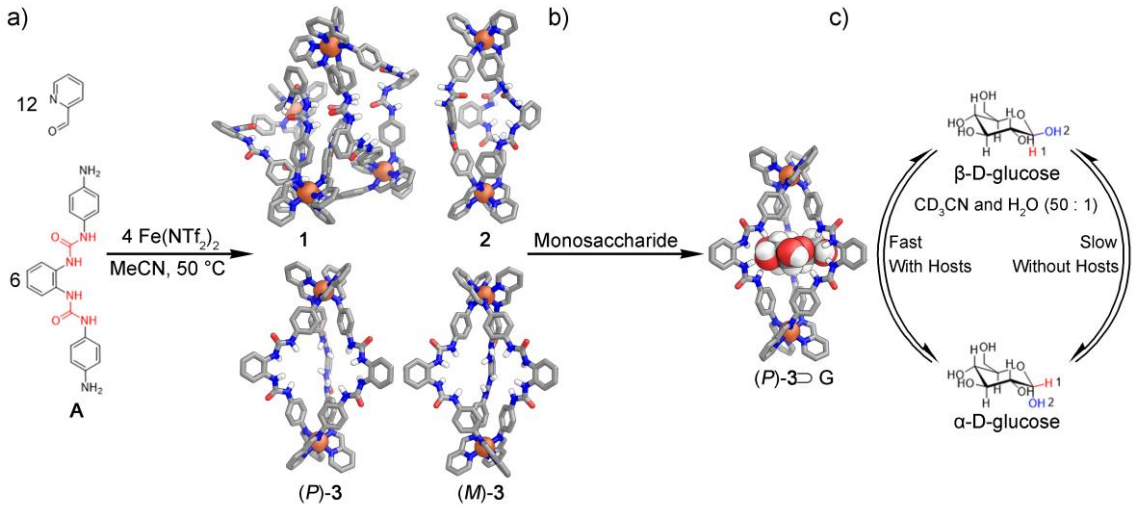

Figure 1. a) Self-assembly of urea-functionalized $Fe^{II}_4L_6$ irregular structure **1**, alongside $Fe^{II}_2L_3$ structures **2** and **3**, from subcomponent **A**, 2-formylpyridine, and iron(II) triflimide. **1** is from the crystal structure, and **2**-**3** are DFT-minimized structures. b) Monosaccharide-induced structural transformation of **1** into $Fe^{II}_2L_3$ structures **2** and **3**. (*P*)-**3**⊃β-D-glucose is illustrated as representative. c) Helicate **3** accelerated the mutarotation of D-glucose.

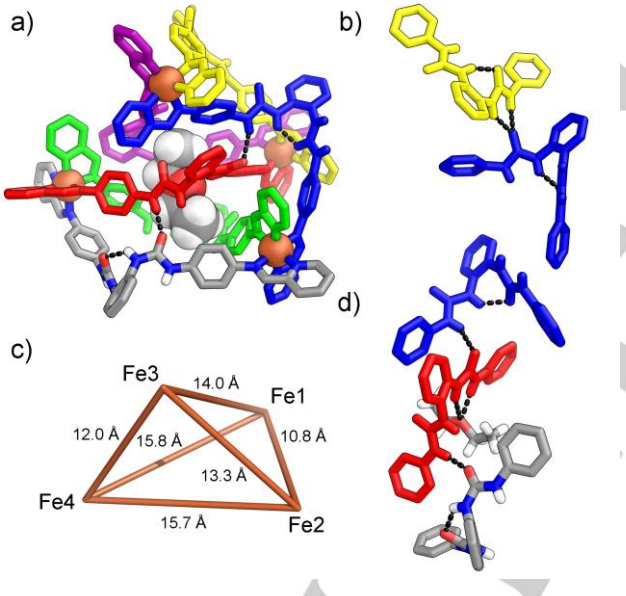

Figure 2. a) Crystal structure of $Fe^{II}_4L_6$ **1** with one Et_2O molecule inside its cavity. b) Intermolecular hydrogen bonding between the urea moieties of **1** in the crystal. c) Distances between the four Fe^{II} vertices. The relative positions of each Fe^{II} are the same in a) and c). d) Examples of the twisted *ortho*-phenylene-bridged bisurea groups, showing intermolecular and intramolecular hydrogen bonding. Hydrogen bonds are depicted as dashed black lines. Only one of the crystallographically unique cations is shown.

The dynamic library of $Fe^{II}_4L_6$ structure **1** and $Fe^{II}_2L_3$ structures **2** and **3** was prepared by the assembly of urea-functionalized subcomponent **A** (6 equiv) and 2-formylpyridine (12 equiv) around iron(II) cations (4 equiv; Figure 1a). Full characterization data for this library are presented in Supporting Information Section S2.2. Irregular structure **1**, mesocate **2** and helicate **3** were observed in solution in a ratio of 35 : 29 : 36 (Figure S4).

The solid-state structure of $Fe^{II}_4L_6$ **1** was determined by single-crystal X-ray measurements[21] (Figure 2; details in Supporting Information Section S7). Three metal centers are facially coordinated (Fe1, Fe3, Fe4), whereas the fourth vertex (Fe2) displays a meridional coordination environment. Two iron(II) centers display Δ (Fe1, Fe2) handedness and the other two are Λ (Fe3, Fe4).

The ligands within the structure adopt a twisted arrangement, resulting in a compact configuration that maximizes hydrogen-bonding but minimizes the cavity volume. One of the ligands, shown in red in Figure 2, threads through the center of the cage, leaving a small cavity occupied by a diethyl ether molecule, with hydrogen bonds (N···O distances 2.88 and 3.26 Å) to two urea NHs. The urea moieties of **1** form multiple intramolecular and intermolecular hydrogen bonds with each other and solvent molecules, with N···heteroatom distances ranging from 2.62 Å to 3.26 Å (Table S6).

As urea-walled organic cages have previously been observed to act as hosts for sugar molecules,[11a] we hypothesized that our assemblies might be suitable hosts for monosaccharides. In the DFT-minimized structures (Figure 1a), the cavities of mesocate **2** and helicate **3** are lined with hydrogen-bond donors pointing into the cavity, providing a complementary environment for the hydrogen-bond accepting groups of monosaccharides. In contrast, twisted **1** lacks such a well-defined cavity.

Thirteen monosaccharide derivatives with different sizes and stereoconfigurations were employed for host-guest studies (Figure 3). ^{1}H NMR spectra revealed evidence of binding to mesocate **2** and helicate **3** for nine of the monosaccharide derivatives (Figures 3a, S29-36). For the other four monosaccharide derivatives (Figure 3b), no evidence for host–guest interaction was observed by ^{1}H NMR (Figures S37-40). Details of chemical shift changes for mesocate **2** and helicate **3** upon guest binding are summarized in Table S1. The imine NMR signals of twisted structure **1** did not shift following addition of any of the monosaccharide derivatives, indicating no interaction between **1** and the prospective guests.

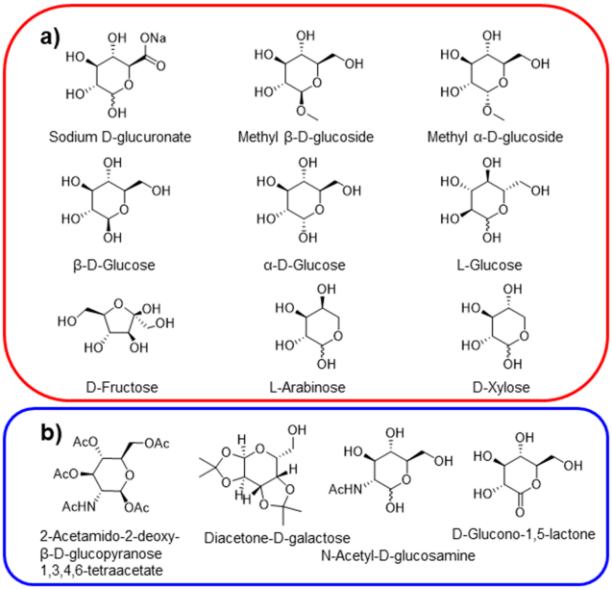

Figure 3. Prospective guests employed in host–guest studies. a) Monosaccharide derivatives which were observed to bind to $Fe^{II}_2L_3$ structures **2** and **3**. b) Monosaccharide derivatives which showed no evidence of interaction with the assemblies.

Upon addition of one of the nine binding monosaccharides (Figure 3a), the relative ^{1}H NMR integrations of the signals corresponding to $Fe^{II}_2L_3$ structures **2** and **3** increased, at the expense of the integrals for $Fe^{II}_4L_6$ **1**. These changes indicated that guests bound exclusively to $Fe^{II}_2L_3$ structures **2** and **3**, and that guest addition resulted in the transformation of non-binding **1** into guest-binding **2** and **3**.

Table 1. Association constants K (M^{-1}) of different monosaccharide derivatives for the $Fe^{II}_2L_3$ structures obtained from ^{1}H NMR titrations (Supporting Information Section S3.2).

Guest	Helicate		Mesocate
	(*P*)–**3**	(*M*)–**3**	**2**
Methyl β-D-glucoside[a]	3820 ± 20	413 ± 2	40[c] ± 3
Methyl α-D-glucoside[a]	266 ± 2	691 ± 2	109[c] ± 1
β-D-Glucose[b]	5920 ± 90	780 ± 20	210 ± 10
α-D-Glucose[b]	780 ± 10	790 ± 10	360 ± 10

[a] measured in CD_3CN. [b] measured in CD_3CN : H_2O = 50 : 1, v/v. [c] association constant too small to be accurately determined by ^{1}H NMR titration.

The binding of three monosaccharide derivatives (α-D-glucose, methyl β-D-glucoside and sodium D-glucuronate) was studied in greater detail (Supporting Information Section S3), providing results consistent with internal binding. To further elucidate the selectivity of guest binding, we investigated the association of the four D-glucopyranose derivatives of Table 1 by ^{1}H NMR titration (Figures S57-S60). Although the sizes and geometries of these monosaccharides are similar, their binding strengths varied significantly.

Upon addition of one of the four D-glucopyranose derivatives, NMR spectra (Figures S57-60) indicated desymmetrization of the hosts framework. Using circular dichroism spectroscopy (CD, discussed below), we assigned the sets of signals for $Fe^{II}_2L_3$ helicate **3** to its ΔΔ (*P*) and ΛΛ (*M*) isomers.

All three $Fe^{II}_2L_3$ stereoisomers (**2**, (*P*)–**3**, and (*M*)–**3**) were observed to bind these guests in a complex competitive equilibrium, precluding the use of a simple 1 : 1 binding isotherm to describe this system.[22] Hence, we developed an extended model accounting for equilibria and guest-binding competition between hosts (Supporting Information Section S3.2), which enabled the extraction of the individual association constants, summarized in Table 1. For a given guest G, this model thus takes into account all of the interlocked equilibria:

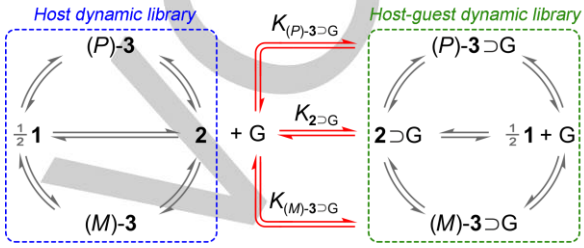

Helicate **3** was a better host for all four guests than mesocate **2**. In particular, (*P*)–**3** preferably bound β-anomeric glycosides over the α-anomers, whereas (*M*)–**3** expressed slightly higher affinity for the α-anomers. The $Fe^{II}_2L_3$ structures, particularly helicate (*P*)–**3**, thus discriminated between guests based upon structural (α/β-anomer) and size (hydroxyl versus methyl substituents) characteristics of the monosaccharides, with (*P*)–**3** showing an order of magnitude stronger affinity for β-D-glucose and β-D-glucoside than for the respective α-anomers.

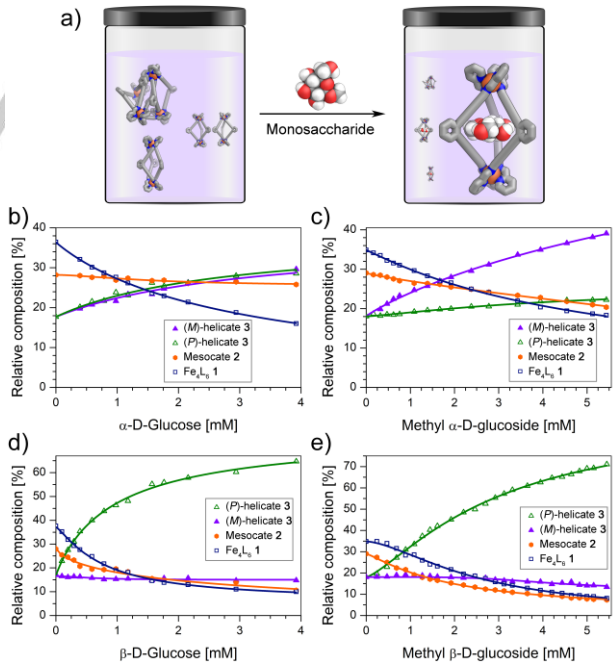

Figure 4. a) Illustration of library redistribution upon guest addition, where size approximates concentration. b-e) The observed and modeled distributions of (*P*)-helicate **3**, (*M*)-helicate **3**, mesocate **2**, and $Fe^{II}_4L_6$ structure **1** upon addition of each of the four different guest molecules b) α-D-glucose, c) Methyl α-D-glucoside, e) β-D-glucose, and f) Methyl α-D-glucoside. ^{1}H NMR titrations were used to calculate the distribution of the structures.

The monosaccharide derivatives altered the distribution between library members upon binding (Figure 4), whereby the strongest-binding host species **3** was amplified within this dynamic combinatorial library.[19] The solvent also affected the equilibrium between **1**, **2** and **3**. These differences were less significant than those imposed by guest binding, however (Figures S4-S26).

We next probed the use of CD measurements for monosaccharide sensing. Following the addition of selected guests (Figure 3a) to the collection of urea-functionalized assemblies, clear CD signals were observed in the range 200-700 nm (Figure 5a) in acetonitrile.

All tested monosaccharides gave rise to distinct CD spectra with the host library (Figure 5b). Sodium D-glucuronate induced the strongest signal. Examination of the sign of the metal-to-ligand charge-transfer (MLCT) transition[23] allowed us to infer that D-glucuronate bound preferentially to, and thus amplified, the $Fe^{II}_2L_3$ structure (*P*)-**3**.[20b, 24] Interestingly, the addition of methyl β-D-glucoside or methyl α-D-glucoside to the system also induced CD spectra, but with absorption features of opposite sign, indicating that the enantiomers of helicate **3** selectively bound the two anomers which further supported our findings from ^{1}H NMR titration studies (Table 1).

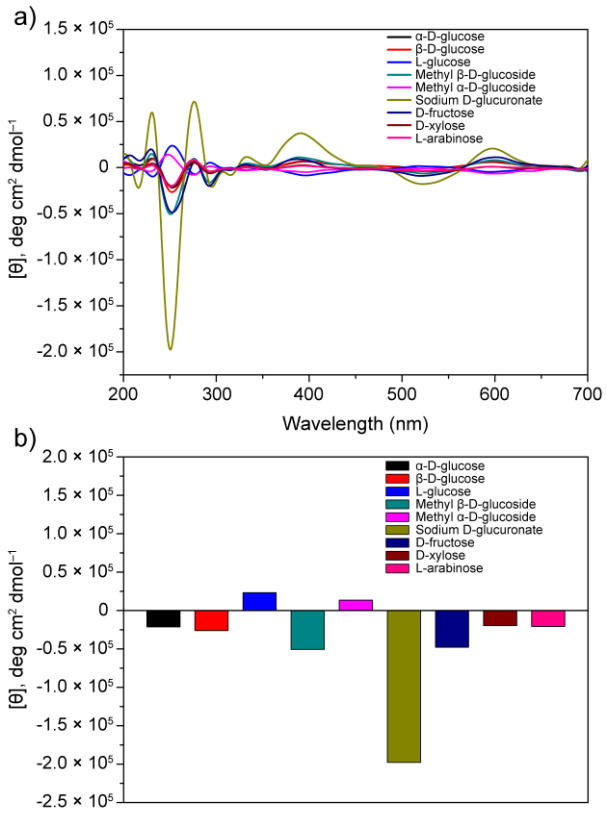

Figure 5. a) Circular dichroism (CD) spectra of the host library with monosaccharide guests in CH_3CN. b) Variation of the CD signal at λ = 250.5 nm with different guests.

A series of kinetic experiments (Supporting Information Section S5) indicated that the library catalyzed mutarotation between α-D-glucose and β-D-glucose, mimicking the catalytic ability of mutarotase.[25] At a total glucose concentration of 1 mM, the barrier to mutarotation $\Delta G^{\ddagger}$ = 83.76 ± 0.08 kJ/mol was determined in the presence of a library of **1**, **2** and **3** having [Fe^{II}] = 2 mM, as compared with a barrier to mutarotation $\Delta G^{\ddagger}$ = 109.87 ± 0.08 kJ/mol (Table S4) in the absence of the library. The presence of the library thus resulted in a 38,000-fold rate enhancement for mutarotation.

Control experiments with $Fe(NTf_2)_2$ and mononuclear Fe^{II} complexes (Supporting Information Section S5) revealed some acceleration of mutarotation, but no change in the equilibrium between α and β glucose. This result supported the hypothesis that trace free Fe^{II}, present due to the dynamic nature of the coordination linkages of the host library, may catalyze the mutarotation of D-glucose. Stronger binding of (*P*)-**3** to β-D-glucose then drove the mutarotation equilibrium towards this anomer. Thus, β-D-glucose and (*P*)-**3** amplified each other in the product mixture, by virtue of their stronger binding to each other, as both host and guest libraries geared together into a single system under equilibrium. The host library both accelerated mutarotation, and changed the equilibrium position between anomers.

Ortho-phenylene-bridged bisurea diamine subcomponent **A** thus generated a library of one $Fe^{II}_4L_6$ and three $Fe^{II}_2L_3$ structures, which possess polar cavities decorated with urea NH hydrogen-bond donors, and interconvert when guest monosaccharides are added that bind to specific library members. The host library was also observed to accelerate the mutarotation of glucose, and specific monosaccharides could be sensed using circular dichroism spectroscopy. Future work on this and related systems may allow them to be developed into practically useful glucose sensors, and to enable the selective functionalization of bound saccharides.

Acknowledgements

This work was supported by the European Research Council (695009) and the UK Engineering and Physical Sciences Research Council (EPSRC EP/P027067/1). The authors thank Diamond Light Source (UK) for synchrotron beamtime on I19 (CY21497). D.Y. acknowledges the National Natural Science Foundation of China (No. 21971210), Natural Science Foundation of Shaanxi Province (2019KJXX-062) and the Chinese Scholarship Council (CSC). L.K.S.v.K. acknowledges the Alexander von Humboldt Foundation for a Feodor Lynen Research Fellowship. J.D.T. acknowledges the Rashkind Family Endowment, the Chenery Endowment, and the Donors of the American Chemical Society Petroleum Research Fund for partial support of this research.

Keywords: glucose binding • dynamic combinatorial library • host–guest systems • metal–organic assemblies • supramolecular chemistry

[1] a) M. Yoshizawa, J. K. Klosterman, M. Fujita, *Angew. Chem., Int. Ed.* **2009**, *48*, 3418-3438; *Angew. Chem*. **2009**, *121*, 3470–3490; b) S. Zarra, D. M. Wood, D. A. Roberts, J. R. Nitschke, *Chem. Soc. Rev.* **2015**, *44*, 419-432; c) C. J. Brown, F. D. Toste, R. G. Bergman, K. N. Raymond, R. G. Bergman, K. N. Raymond, *Chem Rev* **2015**, *115*, 3012-3035; d) Q. Zhang, K. Tiefenbacher, *Nat. Chem.* **2015**, *7*, 197-202; e) S. H. A. M. Leenders, R. Gramage-Doria, B. de Bruin, J. N. H. Reek, *Chem. Soc. Rev.* **2015**, *44*, 433-448.

[2] a) T. Hasell, A. I. Cooper, *Nat. Rev. Mater.* **2016**, *1*, 16053; b) K. Jie, Y. Zhou, E. Li, F. Huang, *Acc. Chem. Res.* **2018**, *51*, 2064-2072; c) P. Howlader, E. Zangrando, P. S. Mukherjee, *J. Am. Chem. Soc.* **2020**, *142*, 9070-9078; d) M. Yamashina, Y. Tanaka, R. Lavendomme, T. K. Ronson, M. Pittelkow, J. R. Nitschke, *Nature* **2019**, *574*, 511-515; e) S. Akine, M. Miyashita, T. Nabeshima, *J. Am. Chem. Soc.* **2017**, *139*, 4631-4634; f) O. Shyshov, R.-C. Brachvogel, T. Bachmann, R. Srikantharajah, D. Segets, F. Hampel, R. Puchta, M. von Delius, *Angew. Chem., Int. Ed.* **2017**, *56*, 776-781; *Angew. Chem*. **2017**, *129*, 794–799.

[3] a) M. J. Webber, R. Langer, *Chem. Soc. Rev.* **2017**, *46*, 6600-6620; b) X. Ma, Y. Zhao, *Chem. Rev.* **2015**, *115*, 7794-7839.

[4] a) G. Zhang, M. Mastalerz, *Chem. Soc. Rev.* **2014**, *43*, 1934-1947; b) I. A. Riddell, M. M. J. Smulders, J. K. Clegg, J. R. Nitschke, *Chem. Commun.* **2011**, *47*, 457-459; c) D. Yang, J. Zhao, Y. Zhao, Y. Lei, L. Cao, X.-J. Yang, M. Davi, N. de Sousa Amadeu, C. Janiak, Z. Zhang, Y.-Y. Wang, B. Wu, *Angew. Chem., Int. Ed.* **2015**, *54*, 8658-8661; *Angew. Chem.* **2015**, *127*, 8782–8785; d) D. Yang, J. Zhao, L. Yu, X. Lin, W. Zhang, H. Ma, A. Gogoll, Z. Zhang, Y. Wang, X.-J. Yang, B. Wu, *J. Am. Chem. Soc.* **2017**, *139*, 5946-5951.

[5] D. M. Rudkevich, In *Functional Synthetic Receptors* (Eds.: T. Schrader, A.D. Hamilton), Wiley-VCH, Weinheim, **2005**, pp. 257-298.

[6] a) R. Chakrabarty, P. S. Mukherjee, P. J. Stang, *Chem. Rev.* **2011**, *111*, 6810-6918; b) S. J. Dalgarno, N. P. Power, J. L. Atwood, *Coord. Chem. Rev.* **2008**, *252*, 825-841; c) N. Kishi, M. Akita, M. Yoshizawa, *Angew. Chem., Int. Ed.* **2014**, *53*, 3604-3607; *Angew. Chem.* **2014**, *126*, 3678–3681; d) D. Zhang, T. K. Ronson, J. R. Nitschke, *Acc. Chem. Res.* **2018**, *51*, 2423-2436; e) Q. Shi, X. Zhou, W. Yuan, X. Su, A. Neniškis, X. Wei, L. Taujenis, G. Snarskis, J. S. Ward, K. Rissanen, J. de Mendoza, E. Orentas, *J. Am. Chem. Soc.* **2020**, *142*, 3658-3670; f) D. Zhang, T. K. Ronson, S. Güryel, J. D. Thoburn, D. J. Wales, J. R. Nitschke, *J. Am. Chem. Soc.* **2019**, *141*, 14534-14538; g) X.-Z. Li, L.-P. Zhou, L.-L. Yan, D.-Q. Yuan, C.-S. Lin, Q.-F. Sun, *J. Am. Chem. Soc.* **2017**, *139*, 8237-8244; h) M. Pan, K. Wu, J.-H. Zhang, C.-Y. Su, *Coord. Chem. Rev.* **2019**, *378*, 333-349; i) C. Tan, D. Chu, X. Tang, Y. Liu, W. Xuan, Y. Cui, *Chem. - Eur. J.* **2019**, *25*, 662-672; j) W. Wang, Y.-X. Wang, H.-B. Yang, *Chem. Soc. Rev.* **2016**, *45*, 2656-2693; k) G. H. Clever, P. Punt, *Acc. Chem. Res.* **2017**, *50*, 2233-2243.

[7] a) J. W. Steed, *Chem. Commun.* **2011**, *47*, 1379-1383; b) M.-O. M. Piepenbrock, G. O. Lloyd, N. Clarke, J. W. Steed, *Chem. Rev.* **2010**, *110*, 1960-2004; c) J. W. Steed, *Chem. Soc. Rev.* **2010**, *39*, 3686-3699.

[8] a) B. Wu, F. Cui, Y. Lei, S. Li, N. d. S. Amadeu, C. Janiak, Y.-J. Lin, L.-H. Weng, Y.-Y. Wang, X.-J. Yang, *Angew. Chem., Int. Ed.* **2013**, *52*, 5096-5100; *Angew. Chem*. **2013**, *125*, 5200–5204; b) S. Li, C. Jia, B. Wu, Q. Luo, X. Huang, Z. Yang, Q.-S. Li, X.-J. Yang, *Angew. Chem., Int. Ed.* **2011**, *50*, 5721-5724; *Angew. Chem*. **2011**, *123*, 5839–5842; c) J. Zhao, D. Yang, X.-J. Yang, B. Wu, *Coord. Chem. Rev.* **2019**, *378*, 415-444; d) D. Yang, J. Zhao, X.-J. Yang, B. Wu, *Org. Chem. Front.* **2018**, *5*, 662-690.

[9] G. Markiewicz, A. Jenczak, M. Kołodziejski, J. J. Holstein, J. K. M. Sanders, A. R. Stefankiewicz, *Nat Commun* **2017**, *8*, 15109.

[10] Y. Liu, W. Zhao, C.-H. Chen, A. H. Flood, *Science* **2019**, *365*, 159-161.

[11] a) R. A. Tromans, T. S. Carter, L. Chabanne, M. P. Crump, H. Li, J. V. Matlock, M. G. Orchard, A. P. Davis, *Nat. Chem.* **2019**, *11*, 52-56; b) Y. Ferrand, M. P. Crump, A. P. Davis, *Science* **2007**, *318*, 619-622; c) A. P. Davis, *Chem. Soc. Rev.* **2020**, *49*, 2531-2545.

[12] Q.-Q. Wang, V. W. Day, K. Bowman-James, *J. Am. Chem. Soc.* **2013**, *135*, 392-399.

[13] D. Zhang, T. K. Ronson, J. Mosquera, A. Martinez, L. Guy, J. R. Nitschke, *J. Am. Chem. Soc.* **2017**, *139*, 6574-6577.

[14] R. Custelcean, P. V. Bonnesen, N. C. Duncan, X. Zhang, L. A. Watson, G. Van Berkel, W. B. Parson, B. P. Hay, *J. Am. Chem. Soc.* **2012**, *134*, 8525-8534.

[15] S. Yi, V. Brega, B. Captain, A. E. Kaifer, *Chem. Commun.* **2012**, *48*, 10295-10297.

[16] L.-P. Zhou, Q.-F. Sun, *Chem. Commun.* **2015**, *51*, 16767-16770.

[17] K. Suzuki, M. Kawano, S. Sato, M. Fujita, *J. Am. Chem. Soc.* **2007**, *129*, 10652-10653.

[18] Q.-Q. Wang, S. Gonell, S. H. A. M. Leenders, M. Düerr, I. Ivanović-Burmazović, J. N. H. Reek, *Nat. Chem.* **2016**, *8*, 225-230.

[19] a) G. Men, J.-M. Lehn, *Chem. Sci.* **2019**, *10*, 90-98; b) J.-M. Lehn, *Chem. Soc. Rev.* **2007**, *36*, 151-160; c) M. Kołodziejski, A. R. Stefankiewicz, J.-M. Lehn, *Chem. Sci.* **2019**, *10*, 1836-1843; d) J. M. Lehn, A. V. Eliseev, *Science* **2001**, *291*, 2331-2332; e) P. T. Corbett, J. Leclaire, L. Vial, K. R. West, J.-L. Wietor, J. K. M. Sanders, S. Otto, *Chem. Rev.* **2006**, *106*, 3652-3711; f) F. B. L. Cougnon, J. K. M. Sanders, *Acc. Chem. Res.* **2012**, *45*, 2211-2221; g) J. Li, P. Nowak, S. Otto, *J. Am. Chem. Soc.* **2013**, *135*, 9222-9239; h) M.-K. Chung, P. S. White, S. J. Lee, M. R. Gagné, *Angew. Chem., Int. Ed.* **2009**, *48*, 8683-8686; *Angew. Chem.* **2009**, *121*, 8839–8842; i) S. M. Voshell, S. J. Lee, M. R. Gagné, *J. Am. Chem. Soc.* **2006**, *128*, 12422-12423; j) B. C. Peacor, C. M. Ramsay, M. L. Waters, *Chem. Sci.* **2017**, *8*, 1422-1428; k) J. F. Reuther, S. D. Dahlhauser, E. V. Anslyn, *Angew. Chem., Int. Ed.* **2019**, *58*, 74-85; *Angew. Chem.* **2019**, *131*, 76–88; l) J. F. Reuther, A. C. Goodrich, P. R. Escamilla, T. A. Lu, V. Del Rio, B. W. Davies, E. V. Anslyn, *J. Am. Chem. Soc.* **2018**, *140*, 3768-3774; m) A. G. Mullins, N. K. Pinkin, J. A. Hardin, M. L. Waters, *Angew. Chem., Int. Ed.* **2019**, *58*, 5282-5285; *Angew. Chem.* **2019**, *131*, 5336–5339; n) L. I. James, J. E. Beaver, N. W. Rice, M. L. Waters, *J. Am. Chem. Soc.* **2013**, *135*, 6450-6455.

[20] The metal centers of dinuclear M_2L_3 complexes may exhibit three combinations of stereochemical configurations (ΔΔ, ΛΛ,) and (ΔΛ) which result in two possible M_2L_3 isomers incorporating achiral ligand **A**: an achiral mesocate **2** (ΔΛ), and the enantiomers of chiral helicate **3** (ΔΔ or ΛΛ). See a) C. Piguet, G. Bernardinelli, G. Hopfgartner, *Chem. Rev.* **1997**, *97*, 2005-2062; b) U. Knof, A. von Zelewsky, *Angew. Chem., Int. Ed.* **1999**, *38*, 302-322; *Angew. Chem*. **1999**, *111*, 312–333; c) J. Xu, T. N. Parac, K. N. Raymond, *Angew. Chem., Int. Ed.* **1999**, *38*, 2878-2882; *Angew. Chem.* **1999**, *111*, 3055–3058.

[21] CCDC 2024202 contains the supplementary crystallographic data for this paper. These data can be obtained free of charge from The Cambridge Crystallographic Data Center.

[22] a) P. Thordarson, *Chem. Soc. Rev.* **2011**, *40*, 1305-1323; b) D. Brynn Hibbert, P. Thordarson, *Chem. Commun.* **2016**, *52*, 12792-12805.

[23] a) S. E. Howson, L. E. N. Allan, N. P. Chmel, G. J. Clarkson, R. van Gorkum, P. Scott, *Chem. Commun.* **2009**, 1727-1729; b) J. L. Bolliger, A. M. Belenguer, J. R. Nitschke, *Angew. Chem., Int. Ed.* **2013**, *52*, 7958-7962; *Angew. Chem*. **2013**, *125*, 8116–8120.

[24] W. Zuo, Z. Huang, Y. Zhao, W. Xu, Z. Liu, X.-J. Yang, C. Jia, B. Wu, *Chem. Commun.* **2018**, *54*, 7378-7381.

[25] S. A. Mulhern, P. H. Fishman, J. W. Kusiak, J. M. Bailey, *J. Biol. Chem.* **1973**, *248*, 4163-4173.

Entry for the Table of Contents

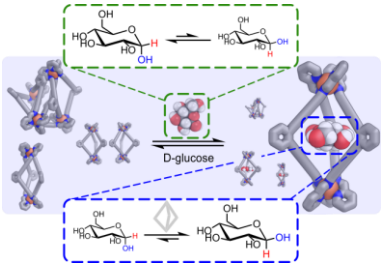

A dynamic library including an $Fe^{II}_4L_6$ irregular structure and three $Fe^{II}_2L_3$ stereoisomers was formed by subcomponent self-assembly. Glucose amplifies the formation of (*P*)-$Fe^{II}_2L_3$ helicate, which in turn amplifies β-D-glucose at the expense of the α-D-anomer. Both host and guest libraries thus geared together into a single system during equilibration.

Institute and/or researcher Twitter usernames: @ChemCambridge, @vkrbek, @JakeyLG ((optional))